Journal of Organometallic Chemistry, 456 (1993) 185–194

JOM 23609

Metal-bridging *vs.* chelating $Me_2Si(C_5H_4)_2$ ligands in dinuclear complexes

III *. Mass spectrometry of organo-rare earth (M = Y, Yb) hydrides containing the $Me_2Si(C_5H_4)_2$ ligand, and crystal structure of the new complex $[\{Me_2Si(\eta^5\text{-}C_5H_4)_2Yb^{III}(THF)\}_2(\mu\text{-}H)(\mu\text{-}Cl)]$

Ke Qiao [1] and R. Dieter Fischer
Institut für Anorganische und Angewandte Chemie der Universität Hamburg, Martin-Luther-King-Platz 6, W-2000 Hamburg 13 (Germany)

Gino Paolucci
Dipartimento di Chimica, Università di Venezia, Calle Larga S. Marta 2137, I-30123 Venezia (Italy)

(Received November 25, 1992)

Abstract

Reactions of $[Me_2Si(C_5H_4)_2MCl]_2$ (Me = CH_3; M = Y, Yb) with NaH in THF have given several new hydride species which have been investigated mainly by high-resolution mass spectrometry (MS). For M = Y, the MS results suggest, as expected, that the reaction gives the dimeric hydride with the ligands $Me_2Si(C_5H_4)_2$ in a chelating mode, while for M = Yb the dimeric species isolated (4) contains only one chlorine and one hydrogen bridging the two Yb atoms. An X-ray crystallographic study of the extremely labile Yb-chloro-hydride crystallized from THF-solution has confirmed the formulation $[\{Me_2Si(C_5H_4)_2Yb(THF)\}_2(\mu\text{-}H)(\mu\text{-}Cl)]$ (4*) with metal-bridging $Me_2Si(C_5H_4)_2$ ligands and one THF ligand on each Yb atom. The unit cell contains two different dimers each of which is accompanied by one additional THF molecule. The starting complex with M = Yb undergoes reversible addition of MeCN, and all its Cl^- ligands may readily be replaced by NCS^- or $[Me_2Si(C_5H_4)_2]^{2-}$.

1. Introduction

Dinuclear organo-f-element complexes containing two closely interlinked cyclopentadienyl ligands, $\{(\mu\text{-}L)(C_5H_4)_2\}^{2-}$ (L = *e.g.* CH_2, SiR_2, etc.), in a metal-bridging, and non-chelating (Fig. 1, isomer a), position have been well-documented but are still comparatively rare [1,3]. Up to now we have mainly been interested in the structural conditions leading to an occasional predominance of isomer a over isomer b [2], and in the application of mass spectrometry (MS) as a potential tool for readily distinguishing the two isomers in the vapour phase [4]. Also of interest, in view of the well-documented catalytic activity of various type b systems [5], is the chemical reactivity of the type a

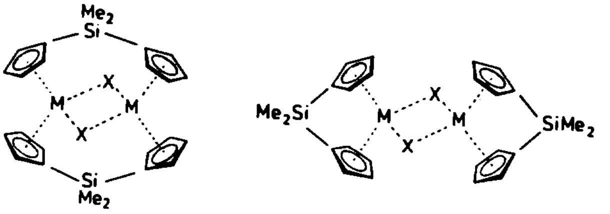

Fig. 1. Isomers of $[R_2Si(C_5H_4)_2M(\mu\text{-}X)]_2$ with metal-bridging (a) and chelating (b) $R_2Si(C_5H_4)_2$ ligands.

Correspondence to: Professor R.D. Fischer or Professor G. Paolucci.

* For Part II, see *J. Organomet. Chem., 408* (1991) 47.

[1] Present address: Institut für Anorganische und Analytische Chemie der Technischen Universität Berlin, Straße des 17. Juni 135, W-1000 Berlin 12 (Germany).

0022-328X/93/$6.00

dimers. Aspects of relevance are whether or not isomer a may coordinate additional ligands and/or undergo exchange of its metal-bridging atoms X without concomitant reorientation of the $Me_2Si(C_5H_4)_2$ ligands from the metal-bridging to the chelating form. Earlier observations had indicated facile cleavage of both the $M \cdots X \cdots M$ and the $M(C_5H_4)Me_2Si(C_5H_4)M$ bridges, *e.g.* by tetrahydrofuran (THF) [1,4], but we now describe some more detailed studies of the reactions of two related $[Me_2Si(C_5H_4)_2M(\mu\text{-}Cl]_2$ systems (with M = Y and/or Yb) with NaH, KNCS and $Na_2[Me_2Si(C_5H_4)_2]$, respectively, as well as with the uncharged potential ligands THF and MeCN.

2. Results and discussion

2.1. Reaction of $[Me_2Si(C_5H_4)_2M(\mu\text{-}Cl)]_2$ (M = Yb: 2; M = Y: 1) with NaH

Solutions of the earlier described compounds $[Me_2Si(C_5H_4)_2M(\mu\text{-}Cl)]_2$ with M = Yb (2 [1]) and Y (1 [2]) in THF were treated at room temperature with an excess of NaH for four days. The pink (M = Yb, product 4) and white (M = Y product 3) powders finally obtained (see Experimental section) both displayed a weak infrared absorption at 2100 cm^{-1} which could, in the absence of ligands involving a triple bond (*e.g.* MeCN, *etc.*), best be associated with partial hydrogenation of silicon atoms, or, less probably, with genuine ν(M–H) absorptions [6*]. The elemental analysis of 4 suggests that only partial substitution of Cl by H atoms may have taken place, but the presence of an unknown amount of THF in 4 (*vide infra*) makes interpretation of the analytical data rather ambiguous.

While the ^1H NMR spectra of 4 and 3 did not help in simulation of these products, the results of MS studies were quite informative. In particular, the presence of dinuclear species still bearing THF-ligands was clearly indicated.

Orange-red, well-shaped crystals of complex (4*) were obtained in good yield after more than one year from a concentrated solution of 4 in THF which had been stored at −30°C. Complex 4* turned out to be extremely sensitive to both traces of oxygen and water and decomposed at temperatures above −20°C, but nevertheless a successful low-temperature single-crystal X-ray study was carried out (*vide infra*). This showed that the composition of product 4* is $[\{Me_2Si(C_5H_4)_2Yb(THF)\}_2(\mu\text{-}H)(\mu\text{-}Cl)] \cdot THF$. The high sensitivity of the crystalline product 4* suggests that, in agreement with their elemental analyses, 4 and 4* differ mainly, if not exclusively, in their THF-contents.

TABLE 1. Summary of crystal data and details of data collection and refinement for 4*

Formula	$C_{36}H_{53}O_3ClSi_2Yb_2$
M (g mol^{-1})	971.52
Crystal dimensions (mm)	0.25 × 0.25 × 0.40
Space group	$Pmc2_1$ (No. 26)
Crystal system	orthorhombic
a/Å	16.300(7)
b/Å	11.506(3)
c/Å	19.676(6)
V/Å^3	3690.0(20)
Z (dimers)	4
D_c (g cm^{-3})	1.749
F(000)	1912
Diffractometer	Enraf-Nonius CAD-4
Temperature (K)	110 ± 5
Radiation λ (Å) [a]	0.71069
Scan technique	ω–2Θ scan
2Θ Range (deg)	$2 \leqslant 2\Theta \leqslant 54$
Number of reflections (total)	4498
Number of reflections (symmetry independent)	3892
Number of reflections (for refinement)	2887 [b]
Number of refined parameters	379
Absorption correction	DIFABS [19]
Absorption coefficient	0.775 (min), 1.075 (max)
Linear absorption coefficient (cm^{-1})	μ = 51.9
Largest peak in final difference Fourier Syntheses (e.Å^3)	1.30
R [c]	0.0399
R_w [d]	0.0360
R_g [e]	0.0394

[a] Mo Kα, graphite monochromator.

[b] $|F_o| \geqslant 4\sigma(F_o)$.

$$R = \frac{\sum \| F_o | - | F_c \|}{\sum | F_o |} \qquad (c)$$

$$R_w = \frac{\sum w^{0.5} \| F_o | - | F_c \|}{\sum w^{0.5} | F_o |} \qquad (d)$$

$$R_g = \left[\frac{\sum w \| F_o | - | F_c \|^2}{\sum w | F_o |^2} \right]^{0.5} \qquad (e)$$

$$w = 1.4922/\left[\sigma^2(F_o) + 0.000309(F_o)^2\right]$$

$$B_{eq} = \tfrac{8}{3}\pi^2 \sum_i \sum_j U_{ij} a_i^* \cdot a_j^* \cdot a_i \cdot a_j$$

$$T = \left[-2\pi^2 \left(U_{11}h^2a^{*2} + U_{22}k^2b^{*2} + U_{33}l^2c^{*2} + 2U_{12}hka^*b^* + 2U_{13}hla^*c^* + 2U_{23}klb^*c^* \right) \right]$$

2.2. Molecular and crystal structure of 4*

Crystal data and details of data collection and refinement are given in Table 1, and the positional parameters in Table 2 and in the supplementary material. There are two slightly different dimers, A and B, and in the asymmetric unit B is accompanied by a disordered lattice-THF molecule. In Fig. 2 an ORTEP

---

* Reference number with an asterisk indicates a note in the list of references.

plot of the molecular structure of A is shown along with the atom numbering scheme. All the Si and methyl C atoms lie, along with the bridging H and Cl atoms, on the only mirror plane of the molecule, the two coordinated THF molecules thus adopting a *cis*oid orientation. Tables 3 and 4 list selected interatomic distances and bond angles in dimers A and B respectively. Figure 3 shows the unit cell.

The most conspicuous feature of 4^* is the presence of one THF ligand on each Yb atom while the initial structure of the dinuclear starting complex **2**, containing two non-chelating $Me_2Si(C_5H_4)_2$ ligands and two metal-bridging Cl atoms [1] is essentially preserved. Facile loss of THF both from the lattice and from the coordination sphere of the sterically congested complexes is expected to be the main reason for the observed instability of the crystals. Both the Yb ··· Yb′ and C(ring)–Yb distances of A and B are not significantly longer than those in **2**, and the O–Yb distances correspond to those of the previously described sterically-congested THF-adducts of organo-Yb complexes [7]. The presence of THF ligands in 4^* leads to a

TABLE 2. Fractional coordinates for non-hydrogen atoms and equivalent isotropic parameters with esd's in parentheses

Atom	*x*	*y*	*z*	B_{eq}
Yb1	0.11663(5)	0.04653(5)	0.50000	1.33
Yb2	0.38370(6)	0.51771(5)	0.25916(4)	1.74
Cl1	0.0000	0.0814(4)	0.4073(2)	1.33
Cl2	0.5000	0.4793(5)	0.1675(3)	2.72
Si1	0.0000	−0.2494(5)	0.4675(3)	1.34
Si2	0.0000	0.2230(5)	0.6377(3)	2.21
Si3	0.5000	0.8045(5)	0.2199(3)	1.47
Si4	0.5000	0.3215(5)	0.3906(3)	1.26
O1	0.1907(6)	0.0657(9)	0.3933(5)	2.16
O2	0.3084(9)	0.4983(10)	0.1536(8)	4.71
O3	0.0000	0.7200(30)	0.7332(20)	14.43
O4	0.5000	0.9120(20)	0.5442(17)	11.13
C1	0.0000	−0.4055(14)	0.4900(11)	1.96
C2	0.0000	−0.2416(18)	0.3752(10)	2.11
C3	0.0951(7)	−0.1811(10)	0.5016(10)	1.46
C4	0.1104(11)	−0.1456(11)	0.5715(7)	1.98
C5	0.1936(11)	−0.1124(13)	0.5767(8)	2.74
C6	0.2265(9)	−0.1199(11)	0.5133(8)	2.01
C7	0.1693(9)	−0.1645(12)	0.4661(8)	1.63
C8	0.0000	0.0992(18)	0.6990(12)	2.73
C9	0.0000	0.3636(17)	0.6872(13)	4.70
C10	0.0941(11)	0.2203(12)	0.5864(7)	2.32
C11	0.1086(10)	0.2713(11)	0.5219(8)	2.14
C12	0.1901(9)	0.2504(11)	0.5040(11)	2.37
C13	0.2298(11)	0.1814(16)	0.5521(9)	3.10
C14	0.1690(12)	0.1653(12)	0.6030(8)	3.15
C15	0.2776(9)	0.0836(13)	0.3916(9)	2.57
C16	0.3119(10)	0.0053(13)	0.3361(10)	3.32
C17	0.2406(10)	0.0114(15)	0.2867(9)	2.98
C18	0.1634(11)	0.0246(15)	0.3259(7)	2.92
C19	0.5000	0.9656(16)	0.2300(11)	2.15
C20	0.5000	0.7830(17)	0.1243(11)	4.43
C21	0.4063(9)	0.7425(10)	0.2577(8)	1.72
C22	0.3295(11)	0.7248(12)	0.2247(12)	3.98
C23	0.2720(11)	0.6836(14)	0.2740(9)	2.99
C24	0.3107(12)	0.6754(14)	0.3345(11)	4.58
C25	0.3931(10)	0.7111(11)	0.3274(8)	2.06
C26	0.5000	0.1726(16)	0.4279(10)	1.48
C27	0.5000	0.4266(16)	0.4645(11)	3.05
C28	0.4053(8)	0.3393(11)	0.3396(6)	1.28
C29	0.3834(11)	0.2898(11)	0.2755(7)	2.07
C30	0.3033(11)	0.3156(12)	0.2591(11)	3.21
C31	0.2728(10)	0.3842(17)	0.3120(13)	5.08
C32	0.3340(9)	0.3957(13)	0.3610(9)	2.61
C33	0.2192(14)	0.5168(16)	0.1498(14)	8.26
C34	0.2110(14)	0.4417(17)	0.0742(11)	4.87
C35	0.2767(18)	0.4320(20)	0.0375(15)	9.53
C36	0.3285(17)	0.4291(19)	0.0949(11)	9.15
C37	−0.0720(13)	0.6572(15)	0.7654(11)	4.09
C38	−0.0472(11)	0.6162(15)	0.8264(9)	3.51
C39	0.5000	0.8760(30)	0.4700(20)	8.72
C40 [a]	0.5191(13)	0.7513(17)	0.4778(11)	0.77
C41 [a]	0.5442(17)	0.7280(20)	0.5223(15)	2.04
C42 [a]	0.5440(18)	0.8170(20)	0.5793(15)	2.12
H101	0.0000	0.0440(40)	0.5037(39)	7.62
H102	0.5000	0.5020(39)	0.3042(37)	0.84

[a] Disordered atoms; probability of occupation: 1/2.

TABLE 3. Selected interatomic distances (Å) in molecules A and B in crystalline 4^* with esd's in parentheses

Molecule A		Molecule B	
Yb(1)–Cl(1)	2.664(3)	Yb(2)–Cl(2)	2.654(4)
Yb(1)–H(101)	1.903(4)	Yb(2)–H(102)	2.10(3)
Yb(1)–O(1)	2.43(1)	Yb(2)–O(2)	2.42(1)
Cl(1)–H(101)	1.95(8)	Cl(2)–H(102)	2.70(8)
Yb(1)–C(3)	2.64(1)	Yb(2)–C(21)	2.61(1)
Yb(1)–C(4)	2.62(1)	Yb(2)–C(22)	2.63(1)
Yb(1)–C(5)	2.68(2)	Yb(2)–C(23)	2.65(2)
Yb(1)–C(6)	2.63(1)	Yb(2)–C(24)	2.63(2)
Yb(1)–C(7)	2.66(1)	Yb(2)–C(25)	2.60(1)
Yb(1)–Z(1) ≠	2.361(6)	Yb(2)–Z(3) ≠	2.336(7)
Yb(1)–C(10)	2.65(1)	Yb(2)–C(28)	2.62(1)
Yb(1)–C(11)	2.63(1)	Yb(2)–C(29)	2.64(1)
Yb(1)–C(12)	2.64(1)	Yb(2)–C(30)	2.67(1)
Yb(1)–C(13)	2.62(2)	Yb(2)–C(31)	2.59(2)
Yb(1)–C(14)	2.59(1)	Yb(2)–C(32)	2.58(2)
Yb(1)–Z(2) ≠	2.334(7)	Yb(2)–Z(4) ≠	2.333(7)
Si(1)–C(1)	1.85(2)	Si(3)–C(19)	1.86(2)
Si(1)–C(2)	1.82(2)	Si(3)–C(20)	1.90(2)
Si(1)–C(3)	1.86(1)	Si(3)–C(21)	1.84(2)
Si(2)–C(8)	1.87(2)	Si(4)–C(26)	1.86(2)
Si(2)–C(9)	1.89(2)	Si(4)–C(27)	1.89(2)
Si(2)–C(10)	1.84(2)	Si(4)–C(28)	1.85(1)
Yb(1)–Yb(1′)	3.802(20)	Yb(2)–Yb(2′)	3.791(20)
Si(1)–Cl(1)	3.986(8)	Si(3)–Cl(2)	3.881(8)
Si(2)–Cl(1)	4.817(8)	Si(4)–Cl(2)	4.750(9)

≠, Ring centre.

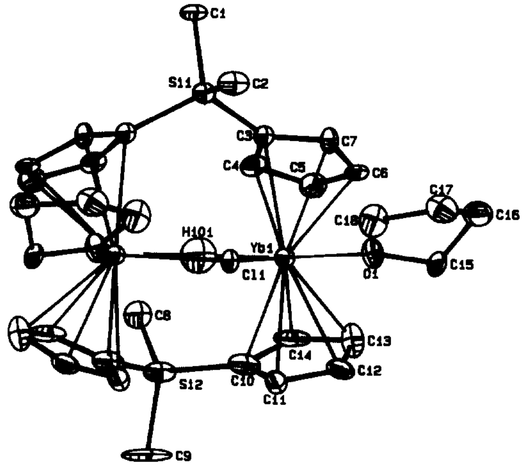

Fig. 2. ORTEP plot of molecule A of 4*.

slightly different arrangement of the two $Me_2Si(C_5H_4)_2$ ligands relative to each other and to the bridging Cl atom from that in **2** and this is reflected in, for example, significantly different values for the distances Si(1)–Cl(1) and Si(2)–Cl(1) and also the distances Si(3)–Cl(2) and Si(4)–Cl(2) (*cf.* Table 3). Complex **2** and its bromine-bridged analogue **5** [2] contain only one crystallographically singular Si atom (but two crystallographically different halogen atoms). As required for metal-bridging $Me_2Si(C_5H_4)_2$ ligands, the angles cent–C(ring)–Si and C(ring)–Si–C(ring)′ are, as in **2** and **5**, significantly larger than 180° and 109.5°, respectively [1,2].

The two molecules A and B differ mainly in the calculated positions of the bridging hydrogen atom, but in view of the presence of rather heavy atoms around the bridging H atom, not too much relevance should be attached to the two different Yb ⋯ H ⋯ Yb′ angles (of 175.0 and 129.0°, *cf.* Table 4). The rather short, albeit different, H ⋯ Cl distances are expected to favour HCl elimination under various constrained conditions. Most other distances and angles in A and B are, however, very similar.

Organo-rare earth complexes involving one halide and one hydride bridge between two metal atoms (i; *cf.* Scheme 1) have been described earlier [8], as have halide-free hydrides also containing THF ligands (ii [9]). However, di- or poly-nuclear systems, which, like

TABLE 4. Selected bond angles (deg) in molecules A and B in crystalline 4* with esd's in parentheses

Molecule A		Molecule B	
Yb(1)–Cl(1)–Yb(1′)	91.0(1)	Yb(2)–Cl(2)–Yb(2′)	91.2(2)
Yb(1)–H(101)–Yb(1′)	175.0(50)	Yb(2)–H(102)–Yb(2′)	129.0(40)
Cl(1)–Yb(1)–H(101)	47.0(20)	Cl(2)–Yb(2)–H(102)	68.0(20)
Cl(1)–Yb(1)–O(1)	75.5(3)	Cl(2)–Yb(2)–O(2)	76.3(4)
Z(1) ≠ –Yb(1)–O(1)	97.2(3)	Z(3) ≠ –Yb(2)–O(2)	96.7(3)
Z(2) ≠ –Yb(1)–O(1)	99.7(3)	Z(3) ≠ –Yb(2)–O(2)	97.4(3)
Z(1) ≠ –Yb(1)–Cl(1)	119.7(2)	Z(3) ≠ –Yb(2)–Cl(2)	120.2(2)
Z(2) ≠ –Yb(1)–Cl(1)	112.9(2)	Z(4) ≠ –Yb(2)–Cl(2)	111.4(2)
Z(1) ≠ –Yb(1)–H(101)	105.6(15)	Z(3) ≠ –Yb(2)–H(102)	104.7(14)
Z(2) ≠ –Yb(1)–H(101)	106.6(17)	Z(4) ≠ –Yb(2)–H(102)	91.5(14)
Z(1) ≠ –Yb(1)–Z(2) ≠	127.2(3)	Z(3) ≠ –Yb(2)–Z(4) ≠	128.4(4)
C(1)–Si(1)–C(2)	106.7(10)	C(19)–Si(3)–C(20)	103.6(9)
C(1)–Si(1)–C(3)	108.8(5)	C(19)–Si(3)–C(21)	110.0(5)
C(2)–Si(1)–C(3)	109.8(7)	C(20)–Si(3)–C(21)	110.5(6)
C(3)–Si(1)–C(3)	112.6(9)	C(21)–Si(3)–C(21)	112.0(9)
C(8)–Si(2)–C(9)	108.7(10)	C(26)–Si(4)–C(27)	106.6(9)
C(8)–Si(2)–C(10)	110.0(6)	C(26)–Si(4)–C(28)	108.4(5)
C(9)–Si(2)–C(10)	107.4(6)	C(27)–Si(4)–C(28)	110.2(5)
C(10)–Si(2)–C(10)	113.2(9)	C(28)–Si(4)–C(28)	112.8(9)
Z(1) ≠ –C(3)–Si(1)	185.2(7)	Z(3) ≠ –C(21)–Si(3)	183.6(8)
Z(2) ≠ –C(10)–Si(2)	181.0(8)	Z(4) ≠ –C(28)–Si(4)	184.7(8)
Dihedral angles			
Yb(1′)–Yb(1)–C(3)–Si(1)	25.4(9)	Yb(2′)–Yb(2)–C(21)–Si(3)	27.6(9)
Yb(1′)–Yb(1)–C(10)–Si(2)	27.7(7)	Yb(2′)–Yb(2)–C(28)–Si(4)	25.2(6)
Angles between planes [a]			
plane(1)------plane(2)	53.1(9)	plane(4)------plane(3)	52.8(9)

[a] Plane(1): {C(3)------C(7)}; plane(2): {C(10)------C(14)}; plane(3): {C(21)------C(25)}; plane(4): {C(28)------C(32)}.

≠ , Ring centre.

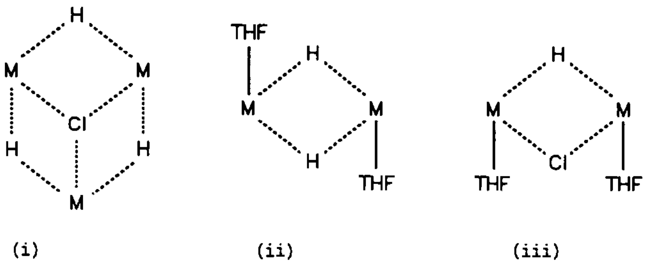

Scheme 1. Reported configurations of tri- and di-nuclear Cp'_2M-derivatives ($Cp' = C_5H_4R$; M = rare earth metal) involving chloride and/or hydride bridges.

4*, involve the skeleton (iii) are to our knowledge unprecedented. A THF-free dimer of major relevance is, however, the complex $[\{Et_2Si(C_5H_4)(C_5Me_4)Lu\}_2(\mu\text{-}Et)]$ [3].

2.3. Mass spectrometry of 4 and 3

As initially the formation of oligomeric, or even polymeric, hydride complexes was envisaged, the mass spectra of the bulk products **4** and **3** were scanned at a relatively high probe temperature (*ca.* 200°C), and the MS results could probably be somewhat improved by use of more appropriate conditions. All fragments with a relative intensity $I_{rel} \geqslant 1\%$ are listed in Tables 5 and 6. Interestingly, in spite of the rather high temperature, both samples give rise to dinuclear fragments involving two or one THF molecule(s), but only **4** displays several dinuclear fragments containing just one Cl atom per dinuclear unit. These findings are in good accordance with the structure revealed by the crystallographic study of **4***. Dinuclear fragments with two Cl atoms are absent from the mass spectra of **4** and **3**, as are other fragments indicative of the presence of un-

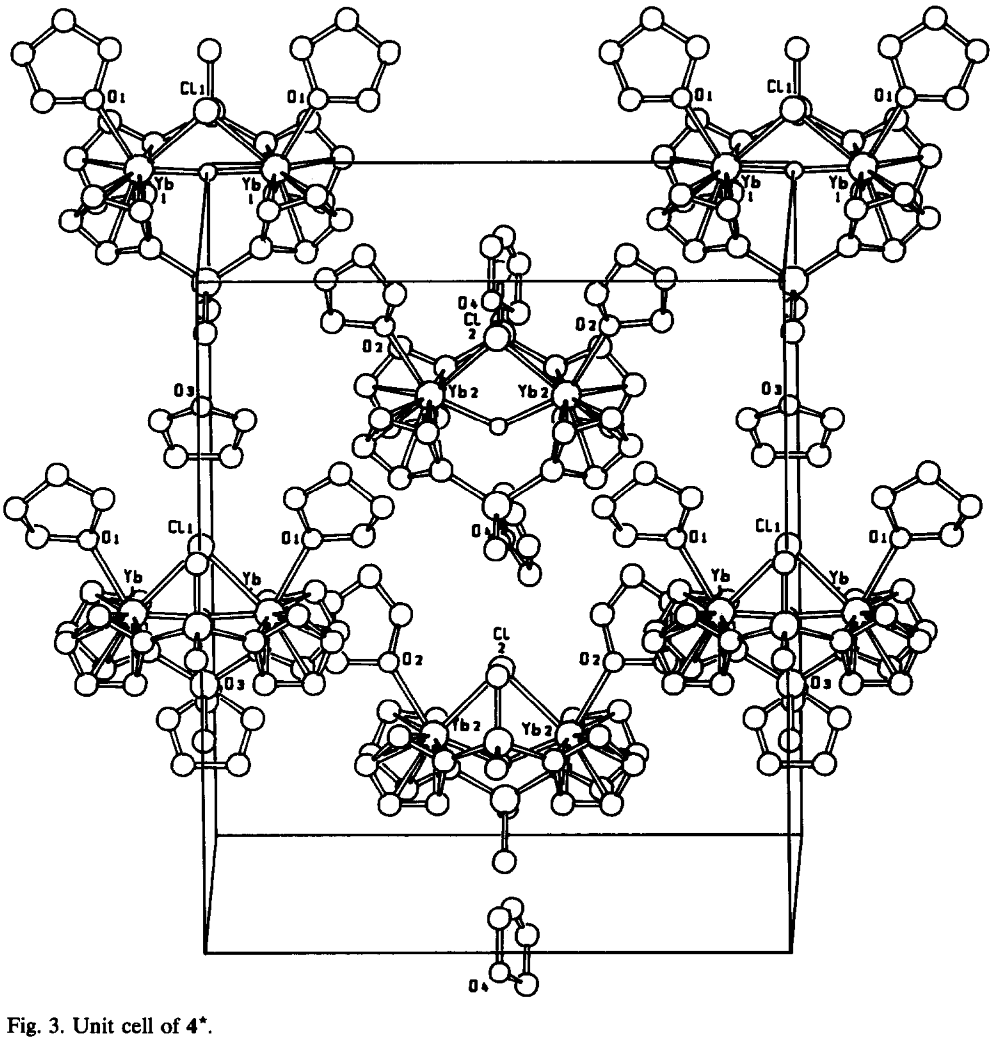

Fig. 3. Unit cell of **4***.

TABLE 5. Composition, m/z (relating to the isotopes ^{35}Cl, ^{28}Si and ^{174}Yb only), and relative abundance of the MS fragments of sample 4 Fragments not containing a metal atom are omitted

Symbol	Formula	m/z	I_{rel}%
$M^{+\cdot}$	$C_{32}H_{45}Si_2O_2ClYb_2$	900	1
$M^{+\cdot}-CH_3\cdot$ (A)	$C_{31}H_{42}Si_2O_2ClYb_2$	885	1
$M^{+\cdot}-THF$	$C_{28}H_{37}Si_2OClYb_2$	828	3
$M^{+\cdot}-C_5H_6$	$C_{27}H_{39}Si_2O_2ClYb_2$	834	5
(A) − THF − Cl·	$C_{27}H_{33}Si_2OYb_2$	777	16
$M^{+\cdot}-2THF$ (B)	$C_{24}H_{29}Si_2ClYb_2$	756	6
(B) − $CH_3\cdot$	$C_{23}H_{26}Si_2O_2ClYb_2$	741	3
(B) − $2CH_3\cdot$	$C_{22}H_{23}Si_2O_2ClYb_2$	726	14
(B) − H· − Cl· (C)	$C_{24}H_{28}Si_2Yb_2$	720	8
(C) − $CH_3\cdot$	$C_{23}H_{25}Si_2Yb_2$	705	26
(C) − $2CH_3\cdot$	$C_{22}H_{22}Si_2Yb_2$	690	18
(B) − C_5H_6 − CH_3 (D)	$C_{18}H_{19}Si_2ClYb_2$	675	9
(D) − H· − Cl·	$C_{18}H_{18}Si_2Yb_2$	639	4
(B) − C_5H_6 − $C_5H_4SiMe_2\cdot$	$C_{12}H_{13}SiClYb_2$	568	12
$[Me_2Si(C_5H_4)_2Yb(C_5H_5)]^{+\cdot}$	$C_{17}H_{19}SiYb$	425	16
$[Me_2Si(C_5H_4)_2YbCl]^{+\cdot}$	$C_{12}H_{14}SiClYb$	395	5
$[Me_2Si(C_5H_4)_2YbH]^{+\cdot}$ [a]	$C_{12}H_{15}SiYb$	361	36
$[Me_2Si(C_5H_4)_2Yb]^{+}$	$C_{12}H_{14}SiYb$	360	100
$[MeSi(C_5H_4)_2Yb]^{+\cdot}$	$C_{11}H_{11}SiYb$	345	30
$[(C_5H_5)_2Yb]^{+\cdot}$	$C_{10}H_{10}Yb$	304	15
$[(C_5H_4)Si(CH_3)CH_2Yb]^{+\cdot}$	C_7H_9SiYb	295	18
$[(C_5H_5)Yb]^{+}$	C_5H_5Yb	239	53

[a] Owing to the presence of seven Yb isotopes, the fragments with and without one extra H atom (*e.g.* $[M^{+\cdot}$ and $M^{+\cdot}-1)$ cannot be identified separately. The shape of the clusters in the experimental spectrum were compared with those simulated by computer.

changed **2** or **1**. Both spectra resemble that of **1** more than that of **2** [4] in that a number of mononuclear fragments also appears. In all cases (except for **2**), the mononuclear fragment: $[C_{12}H_{14}SiM]^+ = [Me_2Si(C_5H_4)_2M]^+$ is the most intense and provides the base peak.

TABLE 6. Composition, m/z (referring to the isotope ^{28}Si only), and relative abundance of the MS fragments of sample 3 Fragments not containing a metal atom are omitted

Symbol	Formula	m/z	I_{rel}%
$M^{+\cdot}$	$C_{32}H_{46}Si_2O_2Y_2$	696	1
$M^{+\cdot}-H\cdot$	$C_{32}H_{45}Si_2O_2Y_2$	695	2
$M^{+\cdot}-2H\cdot$	$C_{32}H_{44}Si_2O_2Y_2$	694	3
$M^{+\cdot}-CH_3\cdot$ (A)	$C_{31}H_{43}Si_2O_2Y_2$	681	3
$M^{+\cdot}-2CH_3\cdot$ (B)	$C_{30}H_{40}Si_2O_2Y_2$	666	4
(A) − THF	$C_{27}H_{35}Si_2OY_2$	609	8
(B) − THF	$C_{26}H_{32}Si_2OY_2$	594	4
$M^{+\cdot}-THF-C_5H_5$	$C_{23}H_{33}Si_2OY_2$	559	8
$M^{+\cdot}-THF-C_5H_6$ (C)	$C_{23}H_{32}Si_2OY_2$	558	2
(C)−H·	$C_{23}H_{31}Si_2OY_2$	557	10
(C) − 2H·	$C_{23}H_{30}Si_2OY_2$	556	2
$M^{+\cdot}-2THF$ (D)	$C_{24}H_{30}Si_2Y_2$	552	3
(D) − H·	$C_{24}H_{29}Si_2Y_2$	551	2
(D) − 2H·	$C_{24}H_{28}Si_2Y_2$	550	5
(D) − $CH_3\cdot$	$C_{23}H_{27}Si_2Y_2$	537	10
(D) − H· − $CH_3\cdot$	$C_{23}H_{26}Si_2Y_2$	536	1
(D) − 2H· − $CH_3\cdot$ (E)	$C_{23}H_{25}Si_2Y_2$	535	3
(D) − $2CH_3\cdot$	$C_{22}H_{24}Si_2Y_2$	522	5
(D) − C_5H_6	$C_{19}H_{24}Si_2Y_2$	486	1
(C) − $Me_2SiH\cdot$	$C_{21}H_{25}SiOY_2$	499	14
(E) − $Me_2Si(C_5H_4)_2$	$C_{11}H_{11}SiY_2$	349	15
$[Me_2Si(C_5H_4)_2Y(C_5H_5)]^{+\cdot}$	$C_{17}H_{19}SiY$	340	8
$[Me_2Si(C_5H_4)_2YH]^{+\cdot}$	$C_{12}H_{15}SiY$	276	19
$[Me_2Si(C_5H_4)_2Y]^{+}$	$C_{12}H_{14}SiY$	275	100
$[MeSi(C_5H_4)_2YH]^{+\cdot}$	$C_{11}H_{12}SiY$	261	7
$[MeSi(C_5H_4)_2Y]^{+}$	$C_{11}H_{11}SiY$	260	3
$[(C_5H_5)_2YH]^{+\cdot}$	$C_{10}H_{11}Y$	220	4
$[(C_5H_5)_2Y]^{+}$	$C_{10}H_{10}Y$	219	21

The existence of only one yttrium isotope allows observation of the loss of one and two hydrogen atoms, respectively, from various dinuclear fragments of **3**, whereas the presence of seven different ytterbium iso-

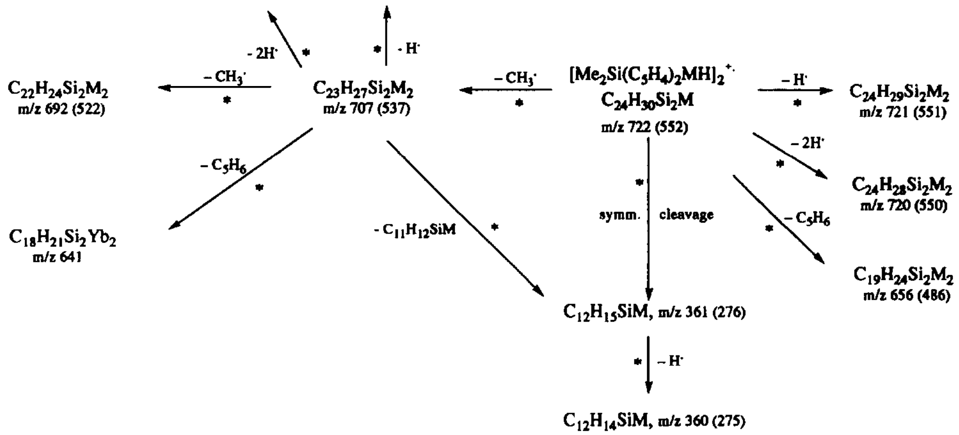

Scheme 2. Detailed B/E-linked scan analysis of the fragments: $[Me_2Si(C_5H_4)_2MH]_2^{+}\cdot$ for M = Yb and (with m/z in parentheses) M = Y. The m/z values refer to the isotopes: ^{28}Si and ^{174}Yb only.

topes gives rise to an extended "isotopic cluster" of signals for each dinuclear fragment. The MS of **3** show various dinuclear fragments that are likely to come successively from the potential molecular ion $[Me_2Si(C_5H_4)_2YH(THF)]_2^{+}\cdot$ at m/z 696. On the other hand, close-lying dinuclear fragments of **4**, whose m/z values would differ by only one or two mass units, cannot be identified with certainty from the ordinary mass spectrum.

The possible presence of a rather weak "isotopic cluster" of **4** centred at $m/z = 722$ was explored by a B/E-linked scan experiment the result of which is summarized in Scheme 2.

The information in Scheme 2 leaves no doubt that there is a fragment centred at m/z 722 that must be assigned to the desolvated dinuclear species $[Me_2Si(C_5H_4)_2YbH]_2^{+}\cdot$. Hence, the presence of small amounts of the Cl-free hydrides $[\{Me_2Si(C_5H_4)_2YbH\}_2(THF)_x]$ in the "bulk product" **4** must also be accounted for. The B/E-linked scan of the expected yttrium analogue of the fragment of **4** at m/z 722 (*i.e.* the fragment of **3** at m/z 552) revealed practically the same fragmentation pathways as depicted for the Yb dimer in Scheme 2. Cleavage of two dinuclear fragments according to Scheme 2 may be one of the sources of the fairly abundant mononuclear fragments, and could, moreover, be considered as evidence for the presence of dinuclear isomers of type b (*cf.* Fig. 1). Several authors have reported that halide-bridged dinuclear dicyclopentadienyl systems devoid of other bridging ligands undergo facile cleavage into mononuclear fragments under MS conditions [10]. The mass spectra of some similar dinuclear hydrides of the type $[(C_5R_5)_2MH]_2$ which display a corresponding cleavage pattern have briefly been reported by Schumann, Marks *et al.* [11]. It is also noteworthy that the bromide-bridged analogue **5** of **2** [2] gives peaks from both di- and mono-nuclear fragments [12].

The mononuclear fragments of **4** and **3** of the composition $[Me_2Si(C_5H_4)_2M(C_5H_5)]^{+}\cdot$ are likely to result from asymmetrical cleavage of a dinuclear parent fragment, involving in addition the breaking of one Si–C(ring) bond and the uptake of one H atom from an adjacent methyl group. The comparatively high intensity of the resulting fragment is in accordance with the usually high stability of tris(cyclopentadienyl) rare earth complexes.

In summary, the MS results of sample **4** agree satisfactorily with the crystallographic findings obtained for complex **4***. On the other hand, the MS data for complex **3** suggest that reaction of **1** with NaH has given mainly the halide-free complex $[Me_2Si(C_5H_4)_2YH]_2$. The apparently different reactions of **2** and **1** with NaH appear to parallel the somewhat different MS properties of these two species [4]. The MS of **1** was interpreted in terms of a facile interconversion of its two isomers a and b (Fig. 1). The presence of substantial amounts of isomer b means that there is more likelihood that mononuclear derivatives will be formed; and these are more susceptible to ligand-exchange reactions.

2.4. Reaction of 2 with KNCS and $Na_2[Me_2Si(C_5H_4)_2]$

The high lability of crystalline **4*** does not rule out the possibility that the bulk material **4** might differ from **4*** also in respect of the bonding mode of the $Me_2Si(C_5H_4)_2$ ligand. In particular, **4** might not necessarily be free of complex units involving chelating $Me_2Si(C_5H_4)_2$ ligands (*i.e.* derivatives of isomer b). The appearance of mononuclear fragments in the mass spectra of **4**, and even more clearly in those of **5**, does not rule out the presence of existing, or easily accessible, mononuclear species in solution. For a further investigation complex **2** was also treated with MeCN, KNCS/NCMe, and $Na_2[Me_2Si(C_5H_4)_2]$/toluene.

While complex **2** is considerably more reluctant to take up acetonitrile than $[(C_5H_4)_2YbCl]_2$ to give the adduct(s) $[Me_2Si(C_5H_4)_2YbCl(NCMe)]_n$ (**6**) with $n = 1$ or 2 [13a,14b], it reacts readily in MeCN with KNCS to the analytically pure derivative $[Me_2Si(C_5H_4)_2Yb(NCS)(NCMe)]_n$ (**7**). The formation of **7** is reminiscent of the similarly spontaneous reaction [13b]:

$$[(C_5H_5)_2YbCl]_2 + 2\,KNCS \xrightarrow{MeCN} 2(C_5H_5)_2Yb(NCS)(NCMe)\ (\mathbf{7a}) + 2\,KCl$$

The similarity of some characteristic features in the infrared data for **7** and **7a** (Table 7) suggests the presence of corresponding structural features in both compounds. The lability of $\mathbf{6} = \mathbf{2}\cdot x$MeCN towards successive losses of nitrile is demonstrated by the appearance of an intense ν(CN) band from free NCMe in the infrared spectrum of a solution of **6** in toluene.

TABLE 7. Comparison of selected infrared absorptions (cm^{-1}) of some adducts containing NCS and/or NCMe ligands

Sample	Vibrations of MeCN (a)	(b)	(c)	Vibrations of NCS ν(CN)	
MeCN [d]	2293	–	2254		
4 [e]	2307	2283	2253		
5	2310	2280	–	2060	1980
5 [a] [13b]	2306	2279	–	2068	1995
4a [f] [13b]	2307	2279	–		

[a] Combination band (Fermi resonance [14]; [b] ν(CN) of coordinated NCMe; [c] ν(CN) of free NCMe; [d] neat liquid; [e] spectrum of toluene solution; [f] $[(C_5H_5)_2YbCl\cdot NCMe]_x$.

We also found that **2** can even react further with $Na_2[Me_2Si(C_5H_4)_2]$ in toluene as follows:

$$[Me_2Si(C_5H_4)_2YbCl]_2 + Na_2[Me_2Si(C_5H_4)_2] \longrightarrow [\{Me_2Si(C_5H_4)_2\}_3Yb_2] + 2\ NaCl$$

The resulting halide-free, viscous oil, **8**, is dark-green in colour, and displays a very similar NIR/Vis absorption spectrum (*ca.* 9000–16000 cm^{-1}) to that of base-free $(\eta^5\text{-}C_5H_5)_3Yb$. In toluene solution the most intense CT band of **8** appears at 14.815 cm^{-1} [$(\eta^5\text{-}C_5H_5)_3Yb$: 15.350 cm^{-1}]. In toluene-d_8, essentially four resonances with strongly temperature-dependent ^1H NMR shifts occur (*cf.* Experimental section), along with two sharper and practically temperature independent proton shifts. In principle, numerous oligomeric, or even polymeric [15a] structures can be envisaged for **8**. Similar mixed-ligand tris(cyclopentadienyl)lanthanoid complexes with a coordinating $(CH_2)_2O(CH_2)_2$ bridge are less difficult to isolate [15b]. Obviously, formation of **8** would be impossible without the rearrangement of at least part of the metal-bridging $Me_2Si(C_5H_4)_2$ ligands of **2** into chelating ligands.

3. Conclusions and suggestions

While dinuclear **2** exchanges only one of its two chloride ligands by a bridging hydride group even in the presence of excess NaH, and can add two molecules of THF to the resulting dimer, **4***, the yttrium homologue, **1**, is more likely to afford a mixture of products dominated by several THF-adducts of the halide-free dinuclear hydride. These findings, which were essentially derived from X-ray and MS studies, are reminiscent of the results of previous comparative MS studies of **2** and **1** [4]. Accordingly, **1** was judged to be a mixture of isomers a and b, while **2** appeared to consist exclusively of isomer a. Our present results seem to confirm that the yttrium dimer, **1**, shows a higher tendency than **2** to give configurations with chelating $Me_2Si(C_5H_4)_2$ ligands derived from isomer b. Alternatively, the barrier of activation for the interconversion: a $\rightleftharpoons$ b may be assumed to be lower for M = Y than for M = Yb. Recently, it has been reported that the mononuclear ferrocenophane, $Me_2Si(C_5H_4)_2Fe$, may be converted into oligo- or polymeric isomers at slightly elevated temperatures (*ca.* 130°C [15]). Therefore, the possibility that partial isomerization might also take place under the conditions in the mass spectrometer cannot be ruled out. Surprisingly, the lutetium homologue of **2**, $[Me_2Si(C_5H_4)_2LuCl]_2$ [16] was found to react with an excess of MeLi in THF to give a colourless halide-free product which did not generate any dinuclear molecules in the vapour phase. Thus, the mass spectrum was fully consistent with the presence of the mononuclear species $Me_2Si(C_5H_4)_2LuMe$. The absence of evidence of any dinuclear precursors suggests that because an excess of MeLi was present formation of the heterodinuclear complex $Me_2Si(C_5H_4)_2Lu(\mu\text{-}Me)_2Li(THF)_x$ was preferred. In keeping with this, we were unable to bring about reaction of this alkyl complex with elemental hydrogen to give the pure hydride $[Me_2Si(C_5H_4)_2LuH]_n$ (with n probably 2 or 3 [17].

As we have pointed out previously [4], the structurally unperturbed $Me_2Si(C_5H_4)_2$ dianion may be regarded as equally unfavorable for chelating and metal-bridging coordination. The present findings simply show once more that various compromises may be reached in situations differing in the nature of the central metal ion and/or of the metal-bridging atoms. The ratio of isomer a- and b-derived species may, moreover, differ with the conditions (*i.e.* crystalline, dissolved, or obtained by evaporation of a solution.

4. Experimental section

All operations were carried out under N_2. All reagent grade chemicals and solvents were rigorously freed from water and oxygen by standard methods. THF-d_8 was dried over potassium ketyl, degassed, and transferred under vacuum.

Infrared spectra were recorded on a Perkin Elmer 325 spectrophotometer. Samples were prepared under a controlled atmosphere in a glove-box as mulls in previously dried and degassed Nujol. ^1H NMR spectra were recorded on a Bruker WP 80 MHz instrument. NIR/VIS spectra were recorded on a Cary 17 spectrophotometer.

All mass spectrometric measurements were carried out on a VG ZAB 2F instrument interfaced with a VG 11/250 data station and operating under electron impact (EI) conditions (70 eV, 200 μA, T(source) = 300°C, T(probe) = 200°C). Samples were introduced by direct probe inlet by use of a device to maintain a vigorous stream of argon around the capillary glass with the sample until the transfer of the sample into the instrument was complete. Metastable transitions were detected by B/E-linked scans [16]. Exact mass measurements were obtained by adopting the peak-matching technique at 10000 resolution power (10% valley definition) only for ions with the monoisotopic rare earth element yttrium as central metal ion.

The starting compounds **2** and **1** were prepared as described in Refs. 1 and 4. The title compound **4** was obtained by stirring a solution of 1.1 g (1.39 mmol) of **2** and 0.09 g (3.75 mmol) of NaH in 50 ml of THF for four hours at room temperature. After complete evaporation of the THF, dissolution of the reddish residue in toluene, and filtration of the solution, the toluene was evaporated off and the pink residue (0.97 g = 96.6% yield) was dried *in vacuo*. Elemental analysis, Calcd. for **4** with and without THF, $C_{32}H_{45}Si_2Yb_2O_2Cl$/$C_{24}H_{29}Si_2Yb_2Cl$: C 42.73/38.17, H 5.04/3.87; Found: C 39.77, H 4.61%. The Y-homologue, **3**, of **4** was prepared correspondingly from 0.8 g (1.39 mmol) of **1** and 0.13 g (5.42 mmol) of NaH. Yield: 0.70 g (98.4%). According to a qualitative analysis, **3** is free of Cl.

4.1. Preparation of 6

A solution of 0.8 g (1.01 mmol) of **2** in 30 ml of acetonitrile was stirred overnight. After complete evaporation of the MeCN, washing of the residue with pentane, and drying *in vacuo*, 0.82 g of a light red powder were obtained. Elemental analysis, calcd. for **2** · 2MeCN: $C_{28}H_{34}N_2Si_2Yb_2Cl_2$: C 38.58, H 3.93, N 3.21. Found: C 35.40, H 4.60, N 1.96%.

4.2. Preparation of $[Me_2Si(C_5H_4)_2Yb(NCS)(NCMe)]_n$ (7)

A solution of 0.406 (0.52 mmol) of **2** and 0.10 g (1.03 mmol) of KNCS in acetonitrile (30 ml) was stirred overnight at room temperature. After filtration, solvent evaporation, and washing of the residue with n-pentane, the pink powder (0.47 g = 99% yield) was dried *in vacuo*. Elemental analysis, Calcd. for $C_{15}H_{17}N_2$ SSiYb: C 39.29, H 3.74, N 6.11. Found: C 39.18, H 3.78, N 5.98% ^1H NMR (toluene-d_8), 335 K: 53.4, −38.0, −17.7, −5.1, +0.91, 1.34 ppm; 210 K: −109.4, −79.5, −71.6, −39.3, +0.97, 1.30 ppm.

4.3. Preparation of $[\{Me_2Si(C_5H_4)_2\}_3Yb_2]$ (8)

A solution of 0.3 g (0.3 mmol) of **2** and 0.09 g (0.38 mmol) of $Na_2[Me_2Si(C_5H_4)_2]$ in 40 ml of toluene was stirred for three days at room temperature. The resulting green solution was filtered (removal of NaCl), and, after solvent evaporation and drying of the residue *in vacuo*, a highly viscous green product (0.2 g = 58.1% yield) remained.

4.4. Crystallographic X-ray study of 4*

A selected orange-red crystal grown from a THF solution at −30°C (the period of crystal growth was *ca.* 15 months) was mounted at low temperature on a glass fibre by using a device introduced by Veith and Bärnighausen [19]. Within the diffractometer, the crystal was continuously exposed to a stream of cold N_2 (temperature 110 ± 5 K). Cell dimensions (*cf.* Table 1) were determined by a least-squares treatment of the setting angles of 25 reflections in the range $17 \leqslant 2\Theta \leqslant 25°$. The selected reflections were controlled for intensity every other hour, and for orientation after every 200 scans. A maximum fluctuation of intensity of −2.2% was observed. Metal atom positions were determined by Patterson mapping using SHELX-86 [20]. The full data set was corrected for polarization, Lorentz, and decay-effects, and an empirical absorption correction was made by use of the program DIFABS [21]. Positional parameters of non-hydrogen and bridging hydrogen atoms are listed in Table 2. The structure was solved by Patterson and difference Fourier methods and refined by full-matrix least-squares optimization of the calculated structure amplitudes (379 parameters) using SHELX-76 [22]. Most of the non-hydrogen atoms were refined anisotropically, while the Yb-bonded H atom and the C atoms of THF were refined isotropically. C_5H_4 ring H atoms were included in the refinement at calculated positions (C–H: 0.95 Å) with a fixed isotropic thermal parameter ($U_{iso,H} = 0.08$ Å^2). The maximal shift for non-H atoms was 0.003 [23*].

Acknowledgments

R.D.F. and K.Q. are grateful for financial support from Deutsche Forschungsgemeinschaft, D.F.G. K.Q. wishes to thank Professor J. Müller (T.U. Berlin) for providing optimal working facilities for him within the framework of a D.F.G.-Graduiertenkolleg. G.P. and R.D.F. thank Dr. P. Traldi and Dr. R. Seraglia (CNR Padua, Italy) for providing access to their mass spectrometers. G.P. is grateful for financial support from the Italian Ministry of Universities and Scientific Research.

References and notes

1 N. Höck, W. Oroschin, G. Paolucci and R.D. Fischer, *Angew. Chem., 98* (1986) 748; *Angew. Chem., Int. Ed. Engl., 25* (1986) 738.

2 T. Akhnoukh, J. Müller, K. Qiao, X.F. Li and R.D. Fischer, *J. Organomet. Chem., 408* (1991) 47.

3 D. Stern, M. Sabat and T.J. Marks, *J. Am. Chem. Soc., 112* (1990) 9558.

4 K. Qiao, R.D. Fischer, G. Paolucci, P. Traldi and E. Celon, *Organometallics, 9* (1990) 1361.

5 (a) G. Jeske, H. Lauke, H. Mauermann, P.N. Swepston, H. Schumann and T.J. Marks, *J. Am. Chem. Soc., 107* (1985) 8091; (b) G. Jeske, H. Lauke, H. Mauermann, H. Schumann and T.J. Marks, *J. Am. Chem. Soc., 107* (1985) 8111; (c) C. Qian, D. Deng, C.-Z. Ni and Z.-M. Zhang, *Inorg. Chim. Acta, 146* (1988) 129.

6 All so far described organolanthanoid hydrides with μ-H ligands display exclusively ν(MH) vibrations at considerably lower wave numbers than 2100 cm^{-1} (*cf.* footnotes 1–12 of ref. 5c).

7 For rather long Yb–O(THF) distances (*i.e.* 2.42–2.46 Å), see: (a) G.B. Deacon, G.D. Fallon and L.D. Wilkinson, *J. Organomet. Chem., 293* (1985) 45; (b) G. Massarweh and R.D. Fischer, *J. Organomet. Chem., 444* (1993) 67.

8 W.J. Evans, J.H. Meadows, A.L. Wayda, W.E. Hunter and J.L. Atwood, *J. Am. Chem. Soc., 104* (1982) 2015.

9 (a) W.J. Evans, J.H. Meadows, W.E. Hunter and J.L. Atwood, *J. Am. Chem. Soc., 106* (1984) 1291; (b) W.J. Evans, J.H. Meadows, W.E. Hunter and J.L. Atwood, *Organometallics, 2* (1983) 1252.

10 (a) J. Müller, *Chem. Ber., 102* (1969) 152; (b) C.-Z. Ni, Z. Zhang, D. Deng and C. Qian, *J. Organomet. Chem., 306* (1986) 209; (c) G. Fu, Y. Xu, Z. Xie and C. Qian, *Acta Chim. Sin., Engl. Edn.*, (1989) 431.

11 G. Jeske, L.E. Schock, P.N. Swepston, H. Schumann and T.J. Marks, *J. Am. Chem. Soc., 107* (1985) 8103.

12 G. Paolucci, R. Seraglia, K. Qiao and R.D. Fischer, in preparation.

13 (a) G. Bielang, Doctoral dissertation, Universität Hamburg (Germany) 1979, p. 18; (b) p. 49.

14 (a) W. Beeckman, J. Goffart, J. Rebizant and M.R. Spirlet, *J. Organomet. Chem., 307* (1986) 23, and literature cited therein; (b) X.-F. Li, S. Eggers, J. Kopf, W. Jahn, R.D. Fischer, C. Apostolidis, B. Kanellakopulos, F. Benetollo, A. Polo and G. Bombieri, *Inorg. Chim. Acta, 100* (1985) 183.

15 (a) D.A. Foucher, B.-Z. Tang and I. Manners, *J. Am. Chem. Soc., 114* (1992) 6246; (b) Q. Qian, Z. Xie and Y. Huang, *J. Organomet. Chem., 398* (1990) 251.

16 K. Qiao and R.D. Fischer, unpublished results.

17 *cf.* $[(1,3\text{-}Me_2C_5H_3)_2Y(\mu\text{-}H)]_3$: W.J. Evans, D.K. Drummond, T.P. Hanusa and R.J. Doedens, *Organometallics, 6* (1987) 2279.

18 A.P. Bruins, K.R. Jenning and S. Evans, *Int. J. Mass Spectrom. Ion Phys., 26* (1978) 395.

19 M. Veith and H. Bärnighausen, *Acta Cryst. Sect. B, 30* (1974) 1806.

20 G.M. Sheldrick, SHELX-86, *Program for Crystal Structure Solution*, Universität Göttingen, Germany, 1986.

21 N. Walker and D. Stuart, *Acta Cryst. Sect. A, 39* (1983) 158.

22 G.M. Sheldrick, SHELX-76, *Program for Crystal Structure Determination*, University of Cambridge, U.K., 1976.

23 Further details of the crystal structure investigation are available on request from the Fachinformationszentrum Energie, Physik, Mathematik GmbH, W-7514 Eggenstein-Leopoldshafen 2, by quoting the depository number, CSD 56718, the names of the authors and the journal citation.